Published in final edited form as:
Hum Mol Genet. 2006 September 15; 15(18): 2825–2835. doi:10.1093/hmg/ddl225.

Expression of the Rho-GEF Pbl/ECT2 is regulated by the UBE3A E3 ubiquitin ligase

Lawrence T. Reiter[1,3], **Tiffany N. Seagroves**[1,2], **Megan Bowers**[1], and **Ethan Bier**[1,*]

[1]Section of Cell and Developmental Biology, University of California, San Diego, 9500 Gilman Dr, Bonner Hall Room 4221, La Jolla, CA 92093, USA

[2]Department of Pathology, University of Tennessee Health Science Center, 855 Monroe Avenue, Memphis, TN 38163, USA

[3]Department of Neurology, University of Tennessee Health Science Center, 855 Monroe Avenue, Memphis, TN 38163, USA

Abstract

We applied genetic tools available in *Drosophila* to identify candidate substrates of the UBE3A ubiquitin ligase, the gene responsible for Angelman syndrome (AS). Human UBE3A was expressed in *Drosophila* heads to identify proteins differentially regulated in UBE3A-expressing versus wild-type extracts. Using two-dimensional gel and MALDI-TOF analysis, we detected 20 proteins that were differentially regulated by over-expression of human UBE3A in *Drosophila* heads. One protein responsive to UBE3A was the Rho-GEF *pebble* (*pbl*). Here, we present three lines of evidence suggesting that UBE3A regulates Pbl. First, we show genetic evidence that UBE3A and the *Drosophila* de-ubiquitinase fat facets (faf) exert opposing effects on Pbl function. Secondly, we find that both Pbl and ECT2, the mammalian orthologue of Pbl called epithelial cell transforming sequence 2 oncogene, physically interact with their respective ubiquitin E3 ligases. Finally, we show that Ect2 expression is regulated by Ube3a in mouse neurons as the pattern of Ect2 expression is dramatically altered in the hippocampus and cerebellum of *Ube3a* null mice. These results suggest that an orthologous UBE3A post-translational regulatory pathway regulates neuronal outgrowth in the mammalian brain and that dysregulation of this pathway may result in neurological phenotypes including AS and possibly other autism spectrum disorders.

Introduction

Angelman syndrome (AS) is a mental retardation disorder characterized by lack of speech, ataxia, and other neurological features (1). The gene affected in AS is the founding member of the E3 ubiquitin ligase family, *UBE3A*. The UBE3A protein product is also known as E6-AP for E6-associated protein (2), but will be referred to herein as UBE3A. *UBE3A* is imprinted in the brains of mice and humans, resulting in expression from the maternal allele only in hippocampal and cerebellar neurons (3). The molecular lesion in ~70% of all AS patients is a deletion encompassing the *UBE3A* gene (4), although maternally inherited point mutations in the *UBE3A* gene also result in an AS phenotype (4). In addition, a maternally derived interstitial duplication of the genomic region encompassing *UBE3A* (15q11–q13) has now been detected in multiple cases of autism spectrum disorder (ASD) (5–7). Involvement of the *UBE3A* gene in the ASD phenotype is likely as there is an

*To whom correspondence should be addressed. Tel: +1 8585348792; Fax: +1 8588222044; ebier@ucsd.edu.

Conflict of Interest statement: The authors have an interest in NovaScape Sciences.

overwhelming preference for maternal but not paternal duplications to cause autism (5,7) and because there is evidence that *UBE3A* is expressed from the duplicated allele (6,8).

Evidence suggests that *UBE3A* function is under tight regulatory control at the epigenetic (9) and post-translational (10) levels in humans, as increasing or decreasing the dosage of this ubiquitin ligase in the brain results in severe mental disabilities ranging from AS to mild forms of autism (11,12). Dysregulation of UBE3A substrates is thought to be the underlying molecular cause for the phenotypes observed in AS and may prove to be the underlying defect in some ASD patients. However, the only well-characterized known substrate of UBE3A is p53 (13), which has not been implicated in the neuronal pathology of ASDs. Therefore, we have taken a combined proteomics and genetic approach to identify additional protein substrates regulated by UBE3A, which might contribute to both AS and ASD phenotypes.

Results

UBE3A has a single *Drosophila* orthologue

Drosophila has a single orthologue of the human *UBE3A* gene (14) (expected value = 102^{-175} given the size of the *Drosophila* genome) (Fig. 1A). The *Drosophila* and human proteins are highly homologous in the C-terminal half of the protein including the enzymatic HECT domain (15). We refer to the *Drosophila* gene [FlyBase (16) ID: CG6190] as *dube3a* for *Drosophila ube3a* gene. Northern blot analysis using a *dube3a* cDNA as probe revealed expression of a ~2.9 kb transcript in embryos, late pupae, and adult heads (Fig. 1B). Subsequent experiments were performed in adult fly heads, which express endogenous *dube3a* and also, presumably, protein substrates of Dube3a.

Two-dimensional gel identification of UBE3A substrates

Human *UBE3A* was cloned into the *Drosophila* GAL4-dependent pUAS expression vector (17) and integrated into the fly genome. We then expressed UBE3A in *Drosophila* heads by crossing lines carrying the UAS-*UBE3A* transgenes to a *Heatshock*-GAL4 (*HS*-GAL4) line, which expresses the yeast GAL4 transactivator protein ubiquitously in response to heat induction. Protein extracts were prepared from adult heads of heat-induced (HS > *UBE3A*) flies and control (*w*-) flies and analyzed by two-dimensional gel electrophoresis. Out of the 400–600 spots visible by silver staining, we identified 20 protein spots that changed markedly in intensity as a result of expressing UBE3A (Table 1). The four most significantly down-regulated protein spots were excised from the gels and analyzed by mass spectrometry (Table 1—spots no. 1, no. 13/14, no. 17 and no. 20). Figure 2 illustrates the elimination of spot no. 1 in response to UBE3A expression (IP = 4.2, MW = 94 kDa), which was identified by mass spectrometry in two independent experiments to be CG8114, the *Drosophila* Rho-guanine-nucleotide exchange factor (Rho-GEF) Pebble (Pbl) (18).

UBE3A can suppress a *GMR > pbl* rough eye phenotype

In order to determine whether putative UBE3A targets might mediate the effects of UBE3A, we asked whether co-expressing *UBE3A* with *pbl* could suppress the rough eye phenotype caused by over-expressing *pbl* in photoreceptor cells (18) with the *G*lass *M*ultimer *R*eporter GAL4 line (*GMR*—GAL4). At 25°C, *GMR* > *pbl* flies have severely disorganized eyes and 40% of the animals display necrotic foci and yellowish loss of pigment at the center of the eye. These flies also have an overall glazed irregular appearance, loss of interommatidial bristles, holes in the lens (Fig. 3B and E, arrowheads), and a severe reduction in the number of photoreceptors (Fig. 3H). In contrast, expression of UAS–*UBE3A* alone with *GMR*–GAL4 had no discernable effect (data not shown, but similar to Fig. 3A, D and G). Co-expression of UBE3A with Pbl reversed much of the effect of *pbl* over-expression. Although

eyes still had a mild rough appearance, fewer than 3% had necrotic foci (Fig. 3C versus B), and the ommatidia were much better organized and well formed than in *GMR > pbl* flies (Fig. 3F versus E), which included six to seven photoreceptors cells per ommatidium (Fig. 3I versus H).

Faf and UBE3A exert opposing effects on pbl

The *Drosophila fat facets* (*faf*) gene encodes a de-ubiquitinating enzyme known to regulate synaptic growth and axon guidance (19,20). Faf also plays an important role in eye morphogenesis (21) that is independent of its function in synapse formation (22). As Faf and Pbl are both known to play a role in axonal pathfinding, we tested whether Faf could antagonize the effects of UBE3A on Pbl. *GMR > pbl* flies have only a weak phenotype (Fig. 4A) at room temperature (RT). *GMR > faf*$^{EP(3)381}$ flies raised at RT have glassy eyes which are also moderately reduced in size (Fig. 4B). The *faf* over-expression phenotype is strongly enhanced by co-expression with *pbl* as the ommatidial field is reduced to ~30% of normal in *GMR > pbl + faf*$^{EP(3)381}$ flies (Fig. 4C). This potent genetic interaction suggests that the de-ubiquitinase Faf acts in part by protecting Pbl from ubiquitin-mediated modification or degradation. The synergistic effect of Pbl and Faf can be overcome by co-expression with UBE3A (Fig. 4D), consistent with UBE3A and Faf exerting opposing activities on Pbl. UBE3A and Faf are also likely to regulate the levels of other proteins essential to normal eye development, as the severe Pbl + Faf phenotype (Fig. 4C) can be almost completely suppressed by UBE3A (Fig. 4D). This strong rescue includes significant suppression of the phenotype caused by Faf expression alone (Fig. 4B).

Co-immunoprecipitation of the E3 ubiquitin ligases and the putative substrates

If Pbl is a direct target of the Dube3a ubiquitin ligase, then these proteins should interact physically. The ability of Pbl to bind to Dube3a was assessed by transient co-transfection of expression plasmids for N-terminally FLAG-tagged Pbl (F-Pbl; ~140 kDa) and N-terminally HA-tagged Dube3a (HA-Dube3a; ~190 kDa) in 293-T cells. A mutant form of Dube3a was also generated, in which a highly conserved Cysteine in the C-terminal enzymatic HECT domain was substituted by Alanine (Dube3a-C/A) (refer to Fig. 1). This mutation in human UBE3A has been previously shown to be capable of binding substrates, but is catalytically inactive with respect to ubiquitin transfer [C833A mutation (23)]. Prior to harvest, transfected cells were treated with the ubiquitin proteasome inhibitor MG-132 to further stabilize potential ligase–substrate interactions. Following immunoprecipitation of whole cell extracts using an α-HA antibody, immunoblots were probed with an α-FLAG antibody. F-Pbl was efficiently precipitated in the presence of either HA-Dube3a wild-type protein or the C/A mutant (Fig. 5A, upper panel, Lanes 5 and 6). As a control, approximately one-fifth of the total amount of lysate used in the IP experiments was resolved on the same gel to confirm expression of F-Pbl (Fig. 5A, upper panel, Lane 7). To confirm expression levels of the HA-tagged Dube3a constructs, this blot was stripped and reprobed with α-HA (Fig. 5A, lower panel). These results indicate that Pbl binds stably to Dube3a in cultured cells, which is consistent with Pbl being a substrate of this E3 ubiquitin ligase.

We next asked if the mammalian orthologue of Pbl [known as epithelial cell transforming sequence 2 oncogene (24) or ECT2] also forms a stable complex with its cognate E3 ubiquitin ligase, human UBE3A. First, 293-T cells were transiently co-transfected with expression constructs for N-terminally FLAG-tagged ECT2 (F-ECT2; ~160kDa) and N-terminally HA-tagged WT UBE3A (HA-UBE3A; ~120 kDa) or the catalytically inactive C833A mutant (HA-UBE3A-C833A) (25). Whole cell extracts were immunoprecipitated with α-Ect2 antibody, followed by western blotting with α-HA (Fig. 5B, upper panel). As in the case of the *Drosophila* orthologues, we found that F-ECT2 co-precipitated both wild-type HA-UBE3A and the enzymatically defective form of UBE3A (C833A) (Fig. 5B, Lanes

5 and 6). We also performed the reciprocal IP in mammalian cells, and as observed with the *Drosophila* proteins, wild-type or mutant HA-UBE3A could co-IP F-Ect2 (data not shown). In addition, because 293-T cells express high endogenous levels of UBE3A, we tested whether transfection of substrate alone (F-Pbl or F-ECT2) was sufficient to observe a physical interaction with UBE3A. Extracts from 293-T cells transfected with either F-ECT2 or F-Pbl were immunoprecipitated with α-UBE3A antibody followed by western blotting for the FLAG epitope. As indicated in Figure 5C, endogenous levels of UBE3A are sufficient to detect interactions with either F-ECT2, or its *Drosophila* orthologue, F-Pbl (Fig. 5C, Lanes 3 and 4). Therefore, the interaction of UBE3A and ECT2/Pbl appears to be conserved between humans and *Drosophila*, which further validates our unique approach of expressing human UBE3A in flies to identify *Drosophila* orthologues of UBE3A substrates.

Ect2 is redistributed in the hippocampus and cerebellum of *Ube3a* null mice

While *Drosophila* is an excellent genetic system for identifying candidate UBE3A substrates, it is essential to validate the relevance of such putative targets in the mammalian brain. We therefore compared the expression pattern of Ect2 in the brains of wild-type and *Ube3a* knockout mice (26). As Ube3a is expressed from the maternal allele only in the hippocampus and Purkinje cells of the mammalian brain (26), we expected that significant changes in Ect2 expression might be observed in these same regions in the $Ube3a^{-/-}$ mouse brain. Ect2 was detected by immunohistochemistry in whole brain sections prepared from age-matched wild-type (+/+) mice or homozygous $Ube3a^{-/-}$ littermates by immunohistochemistry. In wild-type mice, Ect2 was strongly expressed in the same cell layers of the CA3 region in the hippocampus as Ube3a, and in a similar perinuclear pattern (Fig. 6B and E compare with Fig. 6A and D). In contrast, in $Ube3a^{-/-}$ mice, there was a significant increase in overall Ect2 expression in the hippocampus (Fig. 6C versus B) and also a significant expansion of the Ect2 signal into the fiber track layer between CA3 and the dentate gyrus (DG), a region in which there is little expression of either Ube3a or Ect2 in wild-type animals (Fig. 6C versus B, asterisks). In addition, Ect2 no longer appeared to be restricted to a distinct perinuclear pattern as observed in wild-type neurons (Fig. 6E versus F, asterisks). Because localization of Ect2 is altered so pervasively in $Ube3a^{-/-}$ mice, we could not determine from these assays whether the overall expression of Ect2 protein increased at the cellular level. The ectopic Ect2 expression may represent a redistribution of Ect2 protein from the perinuclear region into axonal or dendritic processes of CA3 neurons as well as expression of the protein in fibers originating from other regions of the brain.

Ube3a also regulates Ect2 expression and localization in the cerebellum. We found high levels of Ect2 expression in both the cytoplasm and nucleus of Purkinje cells (Fig. 6H, PL), whereas Ube3a expression was confined mostly to the cytoplasm (Fig. 6G). Low levels of Ect2 staining were also detectable in the granule cell layer (GL) of wild-type mice (Fig. 6H). In the cerebellum of $Ube3a^{-/-}$ mice, however, there was a pronounced reduction in Ect2 immunoreactivity in the cytoplasm of Purkinje cell bodies and a concomitant modest increase in staining in the inter-neuronal space of the molecular layer (ML) into which the Purkinje cells send their elaborate dendritic arbors (Fig. 6H versus J). As previously reported (26), Ube3a expression was not detected in the cerebellum of *Ube3a* null mice (Fig. 6I). We also observed markedly elevated Ect2 staining in the GL of $Ube3a^{-/-}$ mice within the intracellular regions containing mossy fibers and Purkinje cell axons (Fig. 6J), in contrast to the weak staining in this layer in wild-type mice (Fig. 6H). Additional images from independent immunostaining experiments of both hippocampus and cerebellum available online in the Supplemental data section reinforce this conclusion. Thus, both expression levels and the sub-cellular distribution of Ect2 are regulated by Ube3a in cells of the cerebellum and/or hippocampus.

Discussion

Previous studies have identified protein substrates of the UBE3A ubiquitin protein ligase that are involved in cellular growth and cell division [reviewed in ref. (1)], however, none of these substrates seem likely to be responsible for the neurological phenotype observed in AS patients. Here, we have employed a proteomics approach in *Drosophila melanogaster* to identify substrates of the human UBE3A protein. Several potential candidate substrates were identified in our screen and we chose to validate and further characterize one substrate, Pbl/ECT2, a Rho-GEF protein that has been demonstrated to be essential for cytokinesis in both *Drosophila* and in mammalian cells (27). First, and most germane to AS, mutations in Pbl have been shown to affect neuronal outgrowth in post-mitotic cells in *Drosophila* (28). This presumably results from the ability of Pbl to regulate the activity of the small RhoGTPases Rho/Rac/Cdc42, which mediate cytoskeletal remodelling in response to all known neurite guidance cues [reviewed in (29–32)]. Secondly, Ect2 is redistributed between the nucleus (interphase), the cytoplasm (prometaphase) and the midbody (cytokinesis) in cultured HeLa cells (33), suggesting that Ect2 redistribution could also occur in the brain in a regulated manner.

Following identification of Pbl as a UBE3A substrate by proteomic profiling, we demonstrated that expression of UBE3A in the *Drosophila* eye rescues the rough eye phenotype that results from Pbl misexpression. In addition, UBE3A expression reversed the cooperative effects of the de-ubiquitinase Faf and Pbl, suggesting that ubiquitination and de-ubiquitination exert opposing activities on Pbl function during eye development. Next, we demonstrated that Pbl/ECT2 binds directly to endogenous or transfected UBE3A in cultured 293-T cells, consistent with ECT2 activity being regulated directly by UBE3A. We also found that in wild-type mice, Ect2 expression overlaps with that of Ube3a and exhibits a similar perinuclear subcellular localization. More importantly, deletion of *Ube3a* results in mislocalization of Ect2 into ectopic regions within the hippocampus and the cerebellum. Cumulatively, these results suggest that Ube3a is necessary to restrict Ect2 expression to the appropriate cell layers in the brain.

A possible role for ECT2 in learning and behaviour disorders through the regulation of pathfinding or synaptogenesis

Identifying neurologically relevant substrates of the ubiquitin E3 ligase UBE3A is essential to understand the phenotypes associated with AS. However, the results from our study may also have implications for other learning and behavior disorders. For example, maternally derived interstitial duplication of the 15q11-q13 region, which includes the *UBE3A* gene, consistently results in an ASD phenotype. Although there have been rare cases of paternally inherited 15q11-q13 that result in developmental impairments (34,35) there is an overwhelming preference for maternal inheritance of this duplication (5,7,12). This implies that the *UBE3A* gene, which is maternally imprinted in both the hippocampus and cerebellum (3), is likely to be the key gene in this region responsible for the ASD phenotype. We propose, therefore, that at least a subset of idiopathic autism cases may be the result of dysregulation of UBE3A substrates. It may be possible to address this hypothesis by performing association studies on UBE3A substrates like ECT2 in autism families.

ECT2 is the first candidate substrate of UBE3A with an obvious relevance to the neurological phenotypes observed in AS and ASD patients. While the dysregulation of UBE3A substrates like ECT2 in the hippocampus may explain the general learning and behaviour defects observed in both AS and ASD patients, our findings of a Purkinje cell phenotype may provide yet another link between AS and ASD. For example, AS patients exhibit ataxia and motor control problems, which could be explained by the dysregulation of

ECT2 and/or other UBE3A substrates in cerebellum. Similarly, Ahsgren *et al.* (36) found a strong correlation between ASD and non-progressive congenital ataxia, whereas Piek and Dyck (37) found a link between sensory-motor deficits and ASD. Perhaps, more telling in terms of understanding ASD pathology is the possibility that cerebellar defects may explain some of the emotion recognition and expressive language problems observed in ASD individuals (38).

We hypothesize that UBE3A may play a role in regulating growth of neuronal processes or synapse formation through the degradation or cellular localization of various proteins, such as Pbl/ECT2. Our observation that the intracellular distribution of Ect2 is controlled by Ube3a parallels previous studies in which it was observed that Ect2 undergoes a cell cycle-dependent redistribution from the nucleus to cytoplasm, which is controlled by N-terminal sequences distinct from the Rho-GEF domain (18,27). Furthermore, mutations in *pbl* have also been shown to adversely affect neuronal outgrowth in post-mitotic cells, [reviewed in (29–32)]. Thus, gross dysregulation of Pbl may lead to defects in neuronal pathfinding and/or synaptogenesis. Perhaps, UBE3A regulates the sub-cellular localization of ECT2 in post-mitotic neurons to ensure that ECT2 is delivered to the tips of growing axons or dendrites only under appropriate conditions. Given the critical role that Pbl and the Rho/Rac/Cdc42 system plays in axonal navigation and synapse formation in *Drosophila* (39), it seems highly likely that the gross dysregulation of this exquisitely dosage sensitive regulator in the hippocampus and cerebellum of *Ube3a* null mice would result in aberrant neuronal development, connectivity, or function. Such primary phenotypes in turn may underlie part of the observed learning defects and central nervous system features of this murine model for AS. These data are also consistent with growing evidence that the ubiquitin pathway is a key regulator of synaptic growth/stabilization and function (20,22).

It has been reported that activity of ECT2 during G2/M phase of the cell cycle is regulated by phosphorylation (33), however, our data provides the first evidence that ECT2 may also be regulated through the ubiquitin proteasome system via its interaction with UBE3A. One unresolved question is whether ubiquitination of Ect2 would act primarily by marking this protein for degradation, modulating its function or cellular distribution, or whether it acts in both of these capacities. Interestingly, ubiquitination has been implicated in the regulation of both cellular trafficking and intercellular signalling in addition to protein stability (40,41). These recent observations are intriguing in light of our results that cellular distribution of Ect2 was altered in response to deletion of Ube3a in the murine brain. However, it is still not clear whether the levels of Ect2 protein per cell increase substantially overall in *Ube3a*$^{-/-}$ brains since in specific regions, such as the cerebellum or hippocampus, there appears to be substantial redistribution of Ect2 protein into regions in which Ect2 is not detectable in wild-type littermates. Therefore, it is possible that the primary defect in Ect2 regulation in these mice is the cellular relocalization of the UBE3A candidate substrate from the perinuclear region of the cell body to axonal or dendritic processes, rather than control of total protein levels. Further investigation of the role of ubiquitination in regulating Ect2 stability, activity and subcellular localization will be necessary in order to discriminate between these possible mechanisms.

In summary, the combined approach we have taken, which exploits the strengths of both *Drosophila* and mouse models, strongly suggests that Pbl/ECT2 is a direct substrate of the ubiquitin ligase UBE3A and that ECT2 is the most compelling putative substrate identified to date that could be relevant to neurological disorders. Given that increased levels of UBE3A have also been implicated in the pathogenesis of ASD, continued identification and characterization of the multiple substrates regulated by UBE3A in the brain could have far reaching clinical impact for the most common forms of learning defects in humans.

Materials and Methods

Fly stocks and constructs

GAL4 stocks *GMR*–GAL4 and *HS*–GAL4 were provided by the Bloomington Stock Center (Bloomington, IN, USA). Human *UBE3A* (accession no. Q05086) was cloned into the pUAS vector (17). UAS–*pbl* was provided by Bellen (42). The EP line $faf^{EP(3)381}$ was obtained from C. Zucker. All crosses were performed at 25°C except those involving misexpression of $faf^{EP(3)381}$, which were conducted at RT due to the severity of the *GMR*–GAL4 > $faf^{EP(3)381}$ phenotype.

Proteomics

Following a 2 h heat-shock at 38°C, flies were frozen in liquid nitrogen and heads were removed using standard testing sieves of 710 μm followed by 425 μm (Fisher Scientific). Protein extracts for two-dimensional gels and western blot analysis were prepared in standard RIPA homogenization buffer plus EDTA-free protease inhibitors (Roche). For each two-dimensional gel analysis (performed by Kendrick Labs-Madison, WI, USA), 100 μg of total head protein extract was resolved in duplicate on long format gels (MW: 25–400 kDa; pH 3–10). Individual spots were excised and subjected to MALDI-TOF mass spectrometry for protein identification by the Columbia University Proteomics Laboratory.

Northern blot analysis

Total RNA (10 μg) prepared from each tissue was resolved on a denaturing formaldehyde gel, transferred to nylon and probed with P^{32}-labelled cDNA (LD21888 from the *Drosophila* Gene Collection) (43,44), which contains the complete 2.9 kb open reading frame for *dube3a*.

Cell culture expression constructs

Full-length fly *dube3a* was cloned by high fidelity PCR using LD21888 as a template. Amplified product was inserted in-frame with an N-terminal HA epitope that had been previously cloned into the *Kpn*I/*Bam*HI sites of the mammalian expression vector pcDNA3.0. All clones were sequenced to verify that no mutations were generated by PCR. N-terminal HA-tagged WT UBE3A and the C833A mutant cloned into pcDNA3.0 were obtained from the laboratory of Dr Ze'ev Ronai (Burnham Institute, La Jolla, CA, USA). To generate the N-terminal HA-tagged Dube3a-C/A mutant, which mimics the catalytically inactive UBE3A C833A mutation, the most C-terminal Cysteine of Dube3a was mutated by PCR to Alanine via the Quik Change Mutagenesis Kit (Stratagene) using H*A-Dube3a* WT plasmid as a template and clones confirmed by sequencing. Dr Toru Miki (National Institutes of Health, Bethesda, MD, USA) kindly provided the full-length ECT2 construct (pCEV32F3), which contains an N-terminal 3× FLAG epitope (27).

293-T cells transfection and co-immunoprecipitation

293-T cells were maintained in DMEM-Hi medium supplemented with 10% FBS. Confluent 10 cm dishes were passaged at 1:8 on the day prior to transfection. Cells were transfected via FuGene6 (Roche) at a ratio of 3:1 using a total input of 6.0 μg of DNA per 10 cm dish at a 2:1 ratio of ligase (HA-tagged constructs; 4.0 μg input) to FLAG-tagged substrate (F-Pbl or F-ECT2; 2.0 μg). Where indicated, cells were treated with 25 μM MG-132 (Calbiochem) prepared in DMSO for 6 h prior to harvest and were lysed in IP Buffer: 20 mM HEPES pH 7.4, 150 mM NaCl, 0.5% NP-40, 10% Glycerol, 1 mM EDTA, 1 mM EGTA + protease inhibitors. Whole cell extracts (~250 μg) were incubated overnight at 4°C with rotation with either 1.5 μg of α-HA (clone 12CA5, Roche), 1.5 μg of α-UBE3A (Pharmingen, cat. no. 611417) or 2.0 μg of α-Ect2 (Santa Cruz, C-20, sc-1005) antibodies, and then exposed to 10

μl of pre-washed Sepharose G beads (Pierce) for 10 min at RT. The complexes were washed three times with IP lysis buffer, followed by a final wash with IP lysis buffer supplemented with 0.5 m NaCl. Beads were transferred to a fresh tube during the final wash step. Samples were eluted by boiling in 4× sample loading buffer (Invitrogen) and the entire eluate was loaded onto a SDS– PAGE gel for subsequent Western blot analysis with a-FLAG antibody (Sigma, clone M2, F-1804) at 1:5000 or a-HA antibody (12CA5 clone; Roche) at 1:5000 followed by detection with the appropriate secondary antibody and Amersham ECL Plus reagent. Approximately, one-fifth of the lysate used for IP (50 μg) that was prepared in lysis buffer was also loaded onto the gel as an expression control. In the case of Figure 5B, the whole cell lystate was supplemented with NaCl to a final concentration of 0.5 M prior to loading (Fig. 5B). To confirm expression levels of transfected plasmids, blots were stripped and re-probed with either α-HA or α-FLAG antibodies.

Histology

Ube3a wild-type and null mice (n = 4/genotype) were kindly provided by Dr Arthur Beaudet (Baylor College of Medicine, Houston, TX, USA). The brains from age-matched adult littermate mice were perfused with 4% paraformaldehyde, divided along the midline and each half-fixed overnight in 10% neutral-buffered formalin. For antigen retrieval, 4 μm paraffin-embedded sections were microwaved in 10 mM citrate buffer, (pH 6.0) for 20 min, followed by 20 min of cooling. For the hippocampus, Texas Red or FITC-based tyramide signal amplification (TSA) kits (Perkin-Elmer) were used to visualize either α-Ube3a (Santa Cruz, sc-8926; 1:200) or α-Ect2 (Santa Cruz, sc-1005; 1:200) staining, respectively. Because of high levels of autofluoresence in the cerebellum, conventional immunohistochemical staining was performed using the same primary antibodies amplified with the appropriate Vector Elite ABC staining kit, and visualized by Vector VIP substrate; sections were counterstained with 0.1% methyl green.

Acknowledgments

The authors wish to thank Drs Hugo Bellen, Arthur Beaudet, Randy Hampton, Michael Karin, Bill McGinnis, Ze'ev Ronai and Steve Wasserman for discussions and critical review of the manuscript. We also thank Dr Hugo Bellen for providing the UAS–*pbl* flies, Dr Toru Miki for providing pCEV32F3, Dr Ze'ev Ronai for HA-tagged UBE3A plasmids and advice in designing the IP experiments, Aaron Laine for co-IP protocols, BD Scientific for providing the human UBE3A antibody, Dr Arthur Beaudet for *Ube3a* null mice, Neil Daener for expert technical assistance with E.M. studies and Ms Molly Jumper for expert technical assistance with IP studies. L.T.R was a fellow of the Cure Autism Now foundation (CAN) and a portion of this work was supported by a CAN pilot research award to L.T.R. This work was funded in part by grants from the Angelman Syndrome Foundation, N.I.H. R01 GM60585, R01 NS29870 and N.S.F. IBN 0120728 to E.B.

References

1. Jiang Y, Lev-Lehman E, Bressler J, Tsai TF, Beaudet AL. Genetics of Angelman syndrome. Am J Hum Genet. 1999; 65:1–6. [PubMed: 10364509]
2. Huibregtse JM, Scheffner M, Howley PM. Cloning and expression of the cDNA for E6-AP, a protein that mediates the interaction of the human papillomavirus E6 oncoprotein with p53. Mol Cell Biol. 1993; 13:775–784. [PubMed: 8380895]
3. Albrecht U, Sutcliffe JS, Cattanach BM, Beechey CV, Armstrong D, Eichele G, Beaudet AL. Imprinted expression of the murine Angelman syndrome gene, *Ube3a*, in hippocampal and Purkinje neurons. Nat Genet. 1997; 17:75–78. [PubMed: 9288101]
4. Fang P, Lev-Lehman E, Tsai TF, Matsuura T, Benton CS, Sutcliffe JS, Christian SL, Kubota T, Halley DJ, Meijers-Heijboer H, et al. The spectrum of mutations in UBE3A causing Angelman syndrome. Hum Mol Genet. 1999; 8:129–135. [PubMed: 9887341]
5. Schroer RJ, Phelan MC, Michaelis RC, Crawford EC, Skinner SA, Cuccaro M, Simensen RJ, Bishop J, Skinner C, Fender D, et al. Autism and maternally derived aberrations of chromosome 15q. Am J Med Genet. 1998; 76:327–336. [PubMed: 9545097]

6. Herzing LB, Cook EH Jr, Ledbetter DH. Allele-specific expression analysis by RNA-FISH demonstrates preferential maternal expression of UBE3A and imprint maintenance within 15q11-q13 duplications. Hum Mol Genet. 2002; 11:1707–1718. [PubMed: 12095913]

7. Cook EH Jr, Lindgren V, Leventhal BL, Courchesne R, Lincoln A, Shulman C, Lord C, Courchesne E. Autism or atypical autism in maternally but not paternally derived proximal 15q duplication. Am J Hum Genet. 1997; 60:928–934. [PubMed: 9106540]

8. Nurmi EL, Bradford Y, Chen Y, Hall J, Arnone B, Gardiner MB, Hutcheson HB, Gilbert JR, Pericak-Vance MA, Copeland-Yates SA, et al. Linkage disequilibrium at the Angelman syndrome gene UBE3A in autism families. Genomics. 2001; 77:105–113. [PubMed: 11543639]

9. Lalande M, Minassian BA, DeLorey TM, Olsen RW. Parental imprinting and Angelman syndrome. Adv Neurol. 1999; 79:421–429. [PubMed: 10514831]

10. Nuber U, Schwarz SE, Scheffner M. The ubiquitin-protein ligase E6-associated protein (E6-AP) serves as its own substrate. Eur J Biochem. 1998; 254:643–649. [PubMed: 9688277]

11. Peters SU, Beaudet AL, Madduri N, Bacino CA. Autism in Angelman syndrome: implications for autism research. Clin Genet. 2004; 66:530–536. [PubMed: 15521981]

12. Jiang YH, Sahoo T, Michaelis RC, Bercovich D, Bressler J, Kashork CD, Liu Q, Shaffer LG, Schroer RJ, Stockton DW, et al. A mixed epigenetic/genetic model for oligogenic inheritance of autism with a limited role for UBE3A. Am J Med Genet. 2004; 131:1–10. [PubMed: 15389703]

13. Scheffner M, Huibregtse JM, Vierstra RD, Howley PM. The HPV-16 E6 and E6-AP complex functions as a ubiquitin-protein ligase in the ubiquitination of p53. Cell. 1993; 75:495–505. [PubMed: 8221889]

14. Reiter LT, Potocki L, Chien S, Gribskov M, Bier E. A systematic analysis of human disease-associated gene sequences in *Drosophila melanogaster*. Genome Res. 2001; 11:1114–1125. [PubMed: 11381037]

15. Schwarz SE, Rosa JL, Scheffner M. Characterization of human hect domain family members and their interaction with UbcH5 and UbcH7. J Biol Chem. 1998; 273:12148–12154. [PubMed: 9575161]

16. Flybase Consortium. The FlyBase database of the Drosophila Genome Projects and community literature. The FlyBase Consortium. Nucleic Acids Res. 1999; 27:85–88. [PubMed: 9847148]

17. Brand AH, Perrimon N. Targeted gene expression as a means of altering cell fates and generating dominant phenotypes. Development. 1993; 118:401–415. [PubMed: 8223268]

18. Prokopenko SN, Brumby A, O'Keefe L, Prior L, He Y, Saint R, Bellen HJ. A putative exchange factor for Rho1 GTPase is required for initiation of cytokinesis in *Drosophila*. Genes Dev. 1999; 13:2301–2314. [PubMed: 10485851]

19. Kraut R, Menon K, Zinn K. A gain-of-function screen for genes controlling motor axon guidance and synaptogenesis in *Drosophila*. Curr Biol. 2001; 11:417–430. [PubMed: 11301252]

20. DiAntonio A, Haghighi AP, Portman SL, Lee JD, Amaranto AM, Goodman CS. Ubiquitination-dependent mechanisms regulate synaptic growth and function. Nature. 2001; 412:449–452. [PubMed: 11473321]

21. Chen X, Zhang B, Fischer JA. A specific protein substrate for a deubiquitinating enzyme: liquid facets is the substrate of Fat facets. Genes Dev. 2002; 16:289–294. [PubMed: 11825870]

22. Fischer JA, Overstreet E. Fat facets does a highwire act at the synapse. Bioessays. 2002; 24:13–16. [PubMed: 11782945]

23. Huibregtse JM, Scheffner M, Howley PM. Localization of the E6-AP regions that direct human papillomavirus E6 binding, association with p53, and ubiquitination of associated proteins. Mol Cell Biol. 1993; 13:4918–4927. [PubMed: 8393140]

24. Miki T, Smith CL, Long JE, Eva A, Fleming TP. Oncogene ect2 is related to regulators of small GTP-binding proteins. Nature. 1993; 362:462–465. [PubMed: 8464478]

25. Huibregtse JM, Scheffner M, Beaudenon S, Howley PM. A family of proteins structurally and functionally related to the E6-AP ubiquitin-protein ligase. Proc Natl Acad Sci USA. 1995; 92:2563–2567. [PubMed: 7708685]

26. Jiang YH, Armstrong D, Albrecht U, Atkins CM, Noebels JL, Eichele G, Sweatt JD, Beaudet AL. Mutation of the Angelman ubiquitin ligase in mice causes increased cytoplasmic p53 and deficits of contextual learning and long-term potentiation. Neuron. 1998; 21:799–811. [PubMed: 9808466]

27. Tatsumoto T, Xie X, Blumenthal R, Okamoto I, Miki T. Human ECT2 is an exchange factor for Rho GTPases, phosphorylated in G2/M phases, and involved in cytokinesis. J Cell Biol. 1999; 147:921–928. [PubMed: 10579713]
28. Prokopenko SN, He Y, Lu Y, Bellen HJ. Mutations affecting the development of the peripheral nervous system in *Drosophila*: a molecular screen for novel proteins. Genetics. 2000; 156:1691–1715. [PubMed: 11102367]
29. Wong K, Park HT, Wu JY, Rao Y. Slit proteins: molecular guidance cues for cells ranging from neurons to leukocytes. Curr Opin Genet Dev. 2002; 12:583–591. [PubMed: 12200164]
30. Settleman J. Rac'n Rho: the music that shapes a developing embryo. Dev Cell. 2001; 1:321–331. [PubMed: 11702944]
31. Meyer G, Feldman EL. Signaling mechanisms that regulate actin-based motility processes in the nervous system. J Neurochem. 2002; 83:490–503. [PubMed: 12390511]
32. Dontchev VD, Letourneau PC. Growth cones integrate signaling from multiple guidance cues. J Histochem Cytochem. 2003; 51:435–444. [PubMed: 12642622]
33. Hara T, Abe M, Inoue H, Yu LR, Veenstra TD, Kang YH, Lee KS, Miki T. Cytokinesis regulator ECT2 changes its conformation through phosphorylation at Thr-341 in G2/M phase. Oncogene. 2006; 25:566–578. [PubMed: 16170345]
34. Veltman MW, Thompson RJ, Craig EE, Dennis NR, Roberts SE, Moore V, Brown JA, Bolton PF. A paternally inherited duplication in the Prader-Willi/Angelman syndrome critical region: a case and family study. J Autism Dev Disord. 2005; 35:117–127. [PubMed: 15796127]
35. Bolton PF, Veltman MW, Weisblatt E, Holmes JR, Thomas NS, Youings SA, Thompson RJ, Roberts SE, Dennis NR, Browne CE, et al. Chromosome 15q11-13 abnormalities and other medical conditions in individuals with autism spectrum disorders. Psychiatr Genet. 2004; 14:131–137. [PubMed: 15318025]
36. Ahsgren I, Baldwin I, Goetzinger-Falk C, Erikson A, Flodmark O, Gillberg C. Ataxia, autism, and the cerebellum: a clinical study of 32 individuals with congenital ataxia. Dev Med Child Neurol. 2005; 47:193–198. [PubMed: 15739725]
37. Piek J, Dyck M. Sensory-motor deficits in children with developmental coordination disorder, attention deficit hyperactivity disorder and autistic disorder. Hum Mov Sci. 2004; 23:475–488. [PubMed: 15541530]
38. Dyck M, Piek J, Hay D, Smith L, Hallmayer J. Are abilities abnormally interdependent in children with autism? J Clin Child Adolesc Psychol. 2006; 35:20–33. [PubMed: 16390300]
39. Patel BN, Van Vactor DL. Axon guidance: the cytoplasmic tail. Curr Opin Cell Biol. 2002; 14:221–229. [PubMed: 11891122]
40. Haglund K, Di Fiore PP, Dikic I. Distinct monoubiquitin signals in receptor endocytosis. Trends Biochem Sci. 2003; 28:598–603. [PubMed: 14607090]
41. Sun L, Chen ZJ. The novel functions of ubiquitination in signaling. Curr Opin Cell Biol. 2004; 16:119–126. [PubMed: 15196553]
42. Prokopenko SN, Saint R, Bellen HJ. Tissue distribution of PEBBLE RNA and pebble protein during *Drosophila* embryonic development. Mech Dev. 2000; 90:269–273. [PubMed: 10640710]
43. Stapleton M, Carlson J, Brokstein P, Yu C, Champe M, George R, Guarin H, Kronmiller B, Pacleb J, Park S, et al. A *Drosophila* full-length cDNA resource. Genome Biol. 2002; 3:RESEARCH0080. [PubMed: 12537569]
44. Rubin GM, Hong L, Brokstein P, Evans-Holm M, Frise E, Stapleton M, Harvey DA. A *Drosophila* complementary DNA resource. Science. 2000; 287:2222–2224. [PubMed: 10731138]

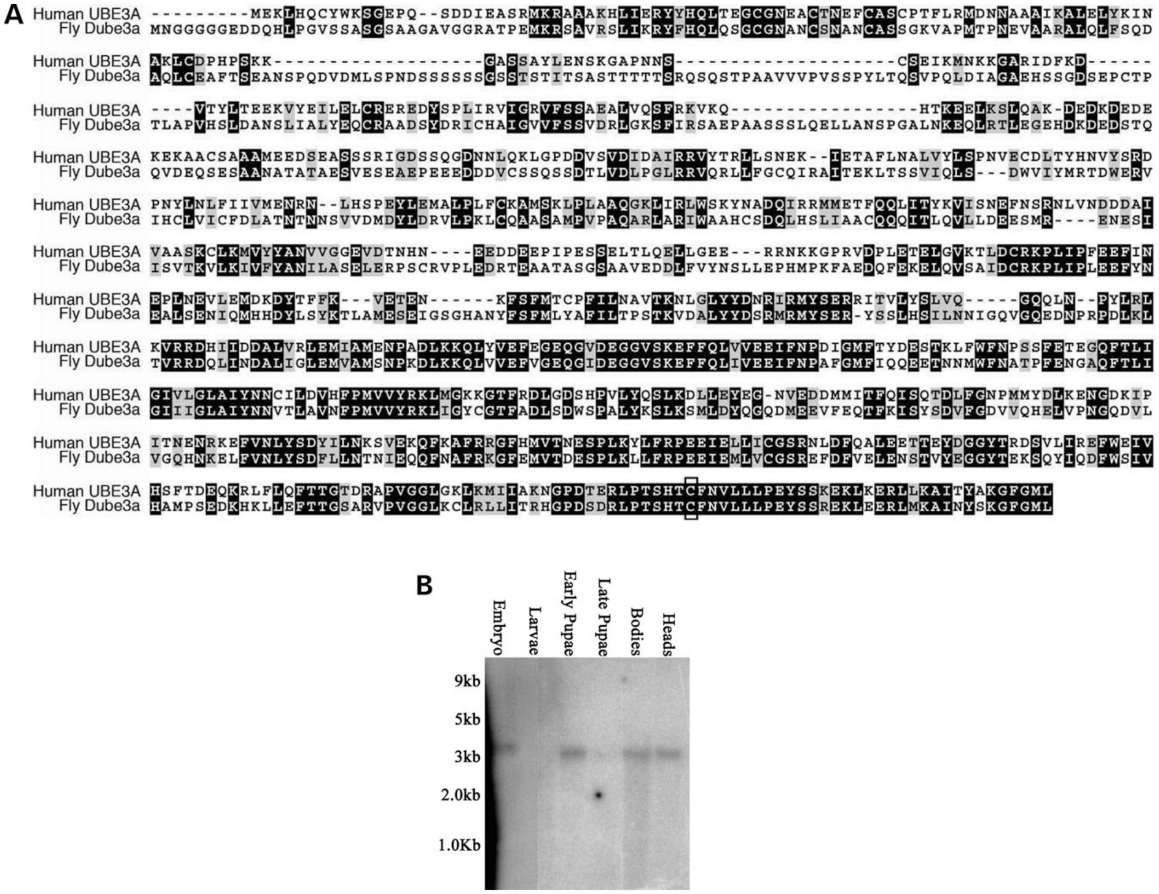

Figure 1.

Identification of *dube3a*, a *UBE3A* homolog in *Drosophila*. (**A**) Amino acid sequence alignment of human UBE3A (accession no. Q05086) with the translated amino acid sequence *of Drosophila* clone LD21888, which encodes a full-length Dube3a protein (FlyBase ID CG6190). Identical residues are outlined in black and conserved residues in dark grey. Although the Dube3a protein displays intermittent homology with UBE3A in the N-terminus of the protein, it matches with greater than 70% sequence identity over the C-terminal half of the coding region that includes the 350 amino acid HECT domain responsible for the transfer of activated ubiquitin from the E2 ligase to the substrate protein (23). The highly conserved C-terminal cysteine residue used to make enzymati-cally inactive forms of UBE3A or Dube3a is outlined with a black box. (**B**) Northern blot identification of *dube3a* transcripts in various tissues using the cDNA LD21888 as a probe. A transcript of the appropriate ~3.6 kb size was detected in *Drosophila* embryos and a slightly smaller ~2.9 kb transcript was also detected in early pupae, adult bodies and adult heads. No *dube3a* transcript was detected in third instar larvae or late pupae. There are three splice-forms of the *UBE3A* transcript in humans, but only one predicted splice form in *Drosophila*.

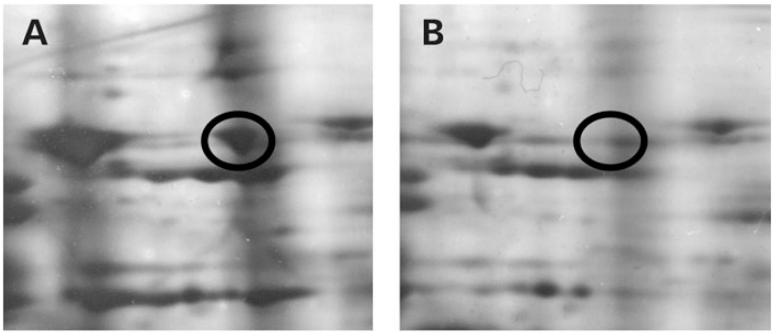

Figure 2.

Two-dimensional gel profiling and GAL4-UAS *Drosophila* protein expression studies. Relevant quadrants of silver-stained two-dimensional gels that contain the spot of interest are presented. The black circle indicates a ~94 kDa protein spot which focused to an isoelectric point (IP) of pH 4.2 in extracts from wild-type heads (**A**). This spot is undetectable at a similar location in the gel in head protein extract from (**B**)*Heatshock*-GAL4 > UAS–*UBE3A* flies (empty black circle). The protein spot identified in (**A**) was partially sequenced by mass spectrometry and was determined in duplicate runs to be the Rho-GEF Pbl [FlyBase (16) ID: CG8114].

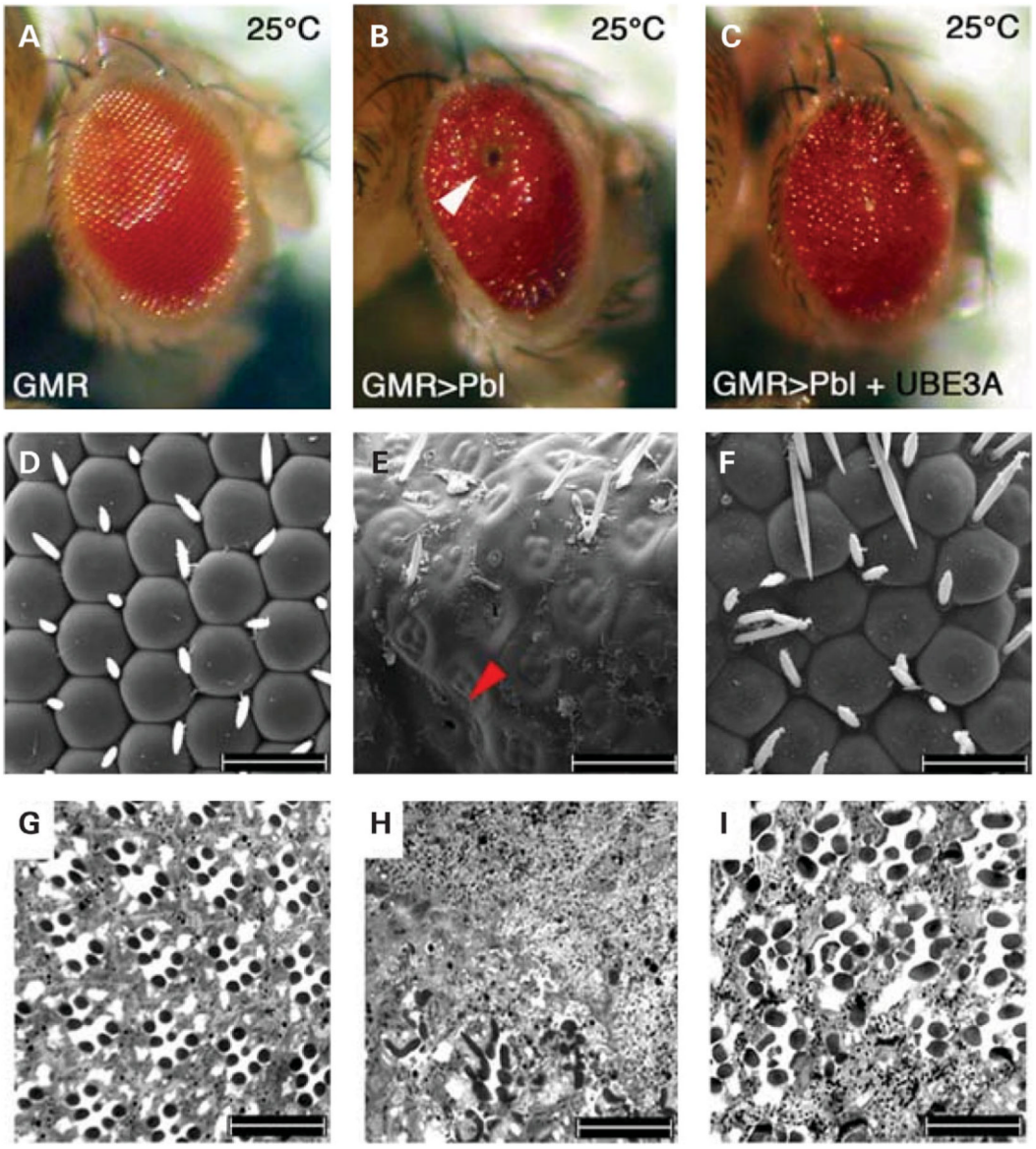

Figure 3.

UBE3A can suppress a Pbl rough eye phenotype. Comparison of *Drosophila* eye phenotypes observed through the dissecting microscope (6.3×; **A–C**), by scanning electron microscopy (1000×; **D–F**), or by transmission electron microscopy on sectioned eyes (1000×; **G–I**). All experiments were performed at 25°C. Scale bar represents 12 μm. (A, D and G) control GMR eyes. Note the regular appearance of single inter-ommatidial bristles in (D) as well as the seven photoreceptor cells visible per ommatidia (G). Expression of human UBE3A alone did not result in any detectable phenotype and is similar to A, D and G (data not shown). (B and E) Over-expression of Pbl at 25°C resulted in a rough eye phenotype with necrotic lesions (white arrow, B) detected in 40.0% of the flies observed ($n = 240$). In addition, the lenses of many individual ommatidia were entirely absent (red arrow, E) and the number of underlying photoreceptor cells were greatly decreased so that many ommatidia were entirely devoid of these cells (H). (C and F) In flies co-expressing human UBE3A with Pbl necrotic foci were detected in only 2.7% of the flies ($n = 332$). Also, the number and size of the ommatidium returned to normal, more inter-ommatidial bristles were present (F compared

with E) and the number of photoreceptor cells per ommatidia increased to at least six, and in some cases to seven per ommatidium.

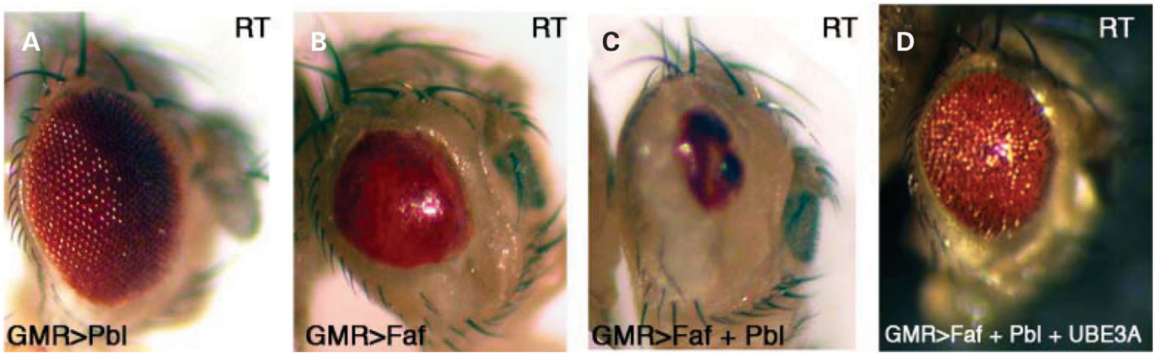

Figure 4.

UBE3A and Faf exert opposing effects on Pbl activity. (**A**) At RT, over-expressing Pbl with *GMR*–GAL4 resulted in a very mild phenotype in 100% of flies, because of the reduced *trans*-activating GAL4 protein activity at lower temperature. (**B**) Over-expression of Faf with *GMR*–GAL4 resulted in a smooth appearance of the eye due to fusion of ommatidia. (**C**) The effect of Faf was strongly enhanced in flies co-expressing Pbl with Faf. (**D**) Co-expression of UBE3A with Faf and Pbl reversed the cumulative effect of Faf + Pbl expression (C), and partially suppressed the smooth eye phenotype induced by expression of Faf alone (B).

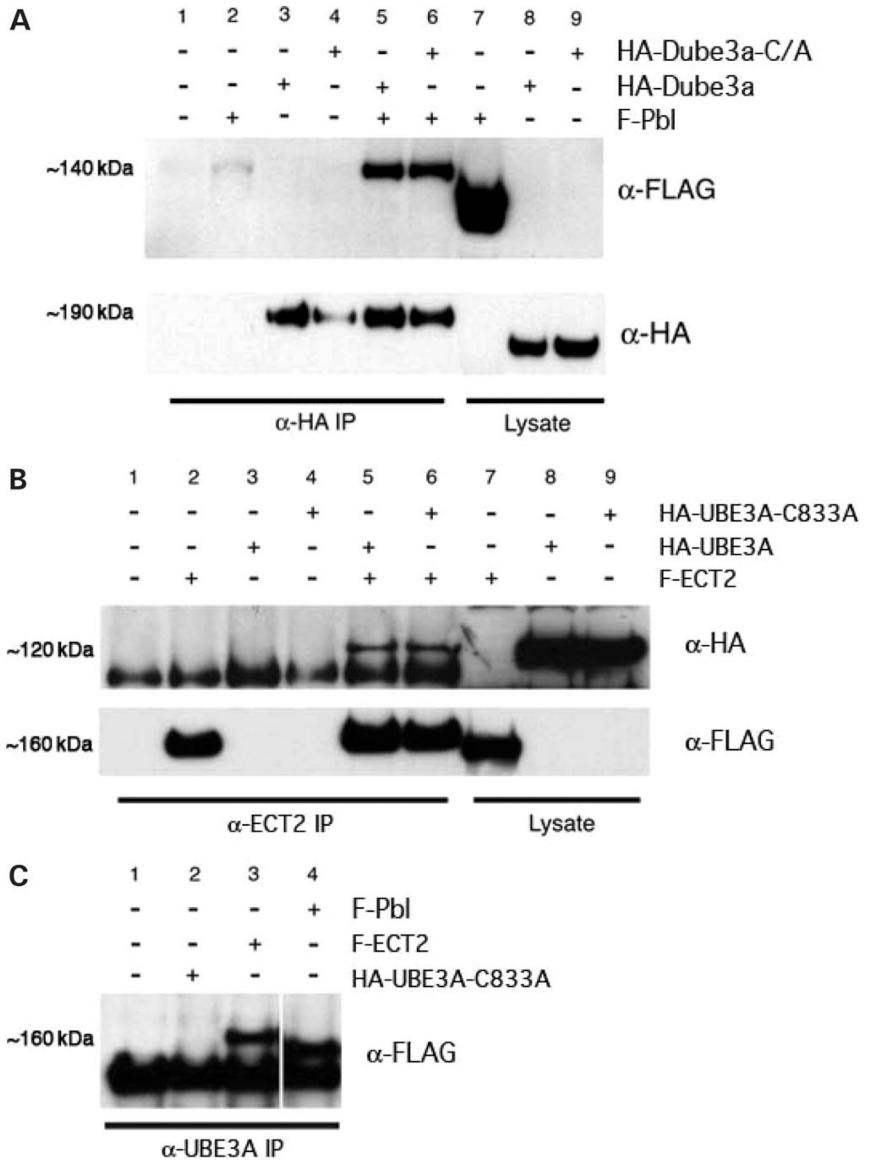

Figure 5.

Dube3a/Pbl and UBE3A/ECT2 associate in human 293-T cells. (**A**) Co-immunoprecipitation of FLAG-Pbl (F-Pbl) with HA-Dube3a (top panel). As controls, human 293-T cells were transiently transfected with either an empty FLAG vector, F-Pbl, HA-Dube3a or the HA-Dube3a-C/A mutant (Lanes 1–4). Co-transfections with F-Pbl and the wild-type or mutant HA-Dube3a ligase (Lanes 5 and 6) were performed as described in the Materials and Methods The ~140 kDa F-Pbl protein was only detected in lanes that contained both the Sepharose G beads and either HA-Dube3a or the HA-Dube3a-C833A mutant. A strong F-Pbl signal could also be detected in whole cell lysates prior to the addition of the beads, although the salt concentration and amount of protein loaded caused the Pbl band to migrate faster than the same protein in the IP lanes ~140 kDa (Lane 7). The faint band observed in Lane 2 (F-Pbl alone) resulted from non-specific binding of the F-Pbl protein extract to the Sepharose G beads, which occurred even in the absence of α-HA antibody bound to the beads (data not shown). The membrane was stripped and re-probed with α-HA antibody (bottom panel). HA-Dube3a was detected at ~190 kDa in Lanes 3, 5

and 8, whereas HA-Dube3a-C/A was detected in Lanes 4, 6 and 9. Once again, the HA-tagged proteins in the lysate (Lanes 8 and 9) migrated faster than the IP lanes because of a difference in salt concentration. (**B**) A similar series of IP experiments was performed using FLAG-tagged ECT2 (F-ECT2) and HA-tagged UBE3A as well as HA-UBE3A-C833A. The ~120 kDa human HA-UBE3A or HA-UBE3A-C833A proteins were only detected following IP with α-Ect2 in samples in which F-ECT2 was also co-transfected (Lanes 5 and 6). HA-tagged UBE3A proteins in the lysate fractions (Lanes 8 and 9) migrated at the same apparent molecular weight as the IP-eluted UBE3A proteins due to supplementation with 0.5 M NaCl prior to electrophoresis. The membrane was stripped and re-probed with α-FLAG antibody (bottom panel). F-ECT2 was detected at ~160 kDa in Lanes 2, 5, 6 and 7. (**C**) Because of high endogenous levels of UBE3A in 293-T cells, it was possible to IP transfected F-ECT2 or F-Pbl using an α-UBE3A antibody without the transfection of additional UBE3A. The ~160 kDa F-ECT2 band (Lane 3) and ~140 kDa F-Pbl protein (Lane 4) were detected by α-FLAG in eluates from an α-UBE3A IP column. Extracts transfected with UBE3A alone (Lane 2) or an empty FLAG vector served as controls (Lane 1).

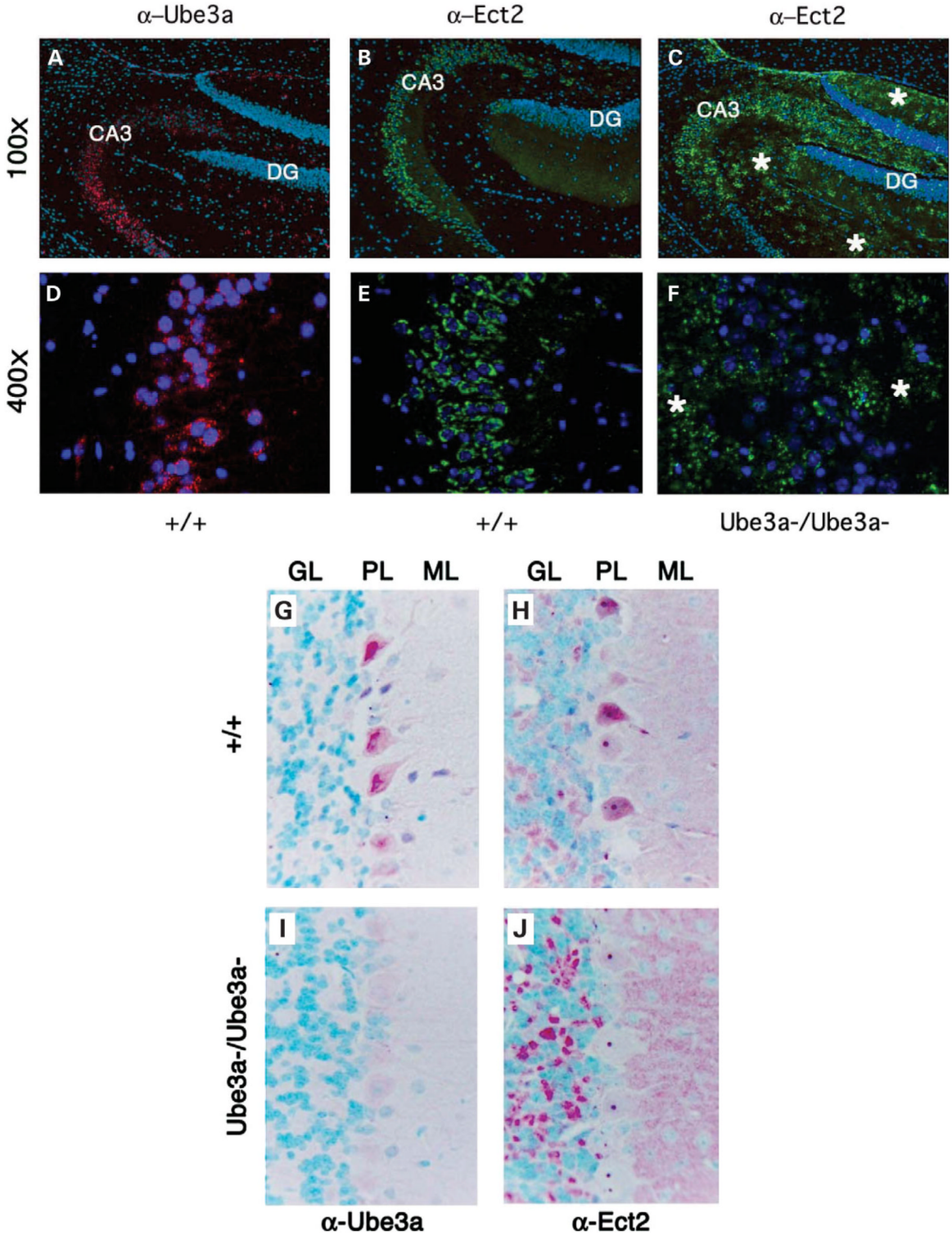

Figure 6.

Ect2 protein expression patterns are altered in the brains of *Ube3a*$^{-/-}$ null mice. Immunohistochemistry was performed on serial paraffin sections from formalin fixed brains isolated from wild-type (**A, B, D** and **E**) or *Ube3a*$^{-/-}$ littermate mice (**C** and **F**) using α-Ube3a (red) or α-Ect2 (green) antisera and counterstaining with DAPI (blue). Images were

captured at either low (100×; A–C) or high power (400×; D–F). (A and D) Ube3a is expressed in a perinuclear staining pattern in wild-type neurons of the CA3 region of the hippocampus (DG is also labelled for reference). (B and E) A similar perinuclear staining pattern was observed for Ect2 in the wild-type hippocampus. Ube3a and Ect2 appear to be expressed in the same cellular layers and regions of the hippocampus. (C and F) Ect2 expression was mislocalized in the hippocampus of *Ube3a*-null animals (compare with B and E in regions with asterisks). In addition, Ect2 could be detected ectopically in layers adjacent to the hippocampus that may reflect a shift in Ect2 localization from the neuronal body in wild-type mice to an axonal and dendritic location in mutant mice (asterisks). (**G–J**) Cerebellar expression of Ube3a (G and I) and Ect2 (H and J) in wild-type (G and H) and *Ube3a* null (I and J) mice. Sections were counterstained with methyl green to identify nuclei. Abbreviations are as follows: GL, granule cell layer; PL, Purkinje cell layer; and ML, molecular cell layer. Both Ube3a and Ect2 proteins are detected in the cytoplasm of Purkinje cell neurons in wild-type mouse brain (G and H). In wild-type mice, Ube3a staining was predominantly confined to the cytoplasm of Purkinje cells (G), whereas Ect2 staining was also detected in the nucleus (H). In contrast, in *Ube3a* null mice Ect2 expression was up-regulated in the intervening space between granule cells, which contains mossy fibers of the granule cell layer and Purkinje cells axons, whereas expression was greatly reduced in the cytoplasm of the Purkinje cell bodies compared with wild-type controls. In the null mice, Ect2 expression was also elevated above wild-type levels within the molecular layer into which the Purkinje cells send their elaborate dendritic arbors (J). No Ube3a staining was detected in either the granule cell layer or the Purkinje cells in the *Ube3a* null mice (I).

Table 1

Molecular weights and isoelectric focusing points for proteins misregulated by UBE3A expression

Spot number	pH	MW (kDa)	Heatshock	Heatshock > UBE3A
1	**4.2**	**94**	**5**	**1**
2	3.8–4.2	90	5	4
3	6.8	90	4	3
4	4	53	5	4
5	4.2	50	2	1
6	7	43	2	1
7	*5.6*	*41*	*3*	*4.5*
8	6	43	3	1
9	4	38	5	3
10	5.25	40	6	4
11	5.8	40	6	5
12	*7.5*	*38*	*1*	*5*
13	**5.5**	**32**	**5**	**1**
14	***5.75***	***32***	***1***	***4.5***
15	6	29	3	1
16	*6.5*	*29*	*1*	*3.5*
17	**6**	**27**	**5**	**1**
18	*3.8*	*28*	*1*	*5*
19	4.5	24	5	4
20	**3.5**	**14**	**4**	**1**

The protein identities of the following two-dimensional gel spots are: #1, pebble; #13/14, a mixture of Δ,5-Δ,2,4-dienoyl-CoA isomerase, carbonic anhydrase (*ca*-1) and oxidoreductase; #17, glutathione transferase; #20, undetermined. Spots in bold text were sent for mass spectrometry analysis and italicized text represents spots that increased in intensity. Spot intensity is indicated on a scale from 5 = dark to 1 = absent.